

# Study of Solvation Dynamics in an Ormosil: CTAB in a Sol–Gel Matrix

Kalyanasis Sahu, Durba Roy, Sudip Kumar Mondal, Arnab Halder, and Kankan Bhattacharyya\*

Physical Chemistry Department, Indian Association for the Cultivation of Science, Jadavpur, Kolkata 700032, India

Received: February 25, 2004; In Final Form: May 20, 2004

Solvation dynamics of coumarin 480 (C480) is studied in a nanoporous sol–gel matrix in the presence of cetyltrimethylammonium bromide (CTAB). In the presence of CTAB, the solvation dynamics is described by two components of 120 ps (25%) and 7200 ps (75%) with a total dynamic Stokes shift of 1200  $\text{cm}^{-1}$ . This is substantially slower than the solvation dynamics in the sol–gel matrix and in CTAB micelles. The anisotropy decay indicates hindered rotation of the probe (C480) inside the sol–gel matrix in the presence of CTAB.

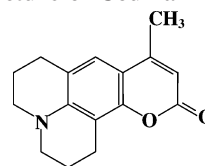
## 1. Introduction

In recent years, there has been a lot of interest in nanoporous inorganic sol–gel matrices.<sup>1</sup> A sol–gel matrix may be obtained quite easily by the hydrolysis of tetra-alkyl orthosilicate.<sup>1</sup> The pore size of a sol–gel matrix may be tuned by pH variation.<sup>1</sup> Hydrolysis in an acidic medium results in small pore sizes (diameter, 1–3 nm), but an alkaline medium produces large pores (diameter 4–200 nm).<sup>1</sup> More recently, many groups have reported on the incorporation of biological macromolecules,<sup>2–4</sup> surfactants,<sup>3b,c</sup> photochromic dyes,<sup>3d</sup> and many other organic additives.<sup>2–8</sup> A sol–gel matrix doped with an organic additive is called an ormosil. The ormosils have versatile applications in the long-term storage of immobilized proteins and biological assemblies in biologically active forms and have been studied by fluorescence spectroscopy.<sup>1a,2–4</sup>

The dynamics of a liquid confined in a sol–gel matrix reveals rich complexity. The hydrolysis of a tetra-alkyl orthosilicate leaves water molecules confined in the sol–gel matrix. The confined water molecules may be removed by heating, and then other liquids may be introduced by simply soaking the “dry” sol–gel glass with other liquids. Many groups used the optical Kerr effect (OKE) to study the dynamics of reorientation of many liquids in a sol–gel glass.<sup>5,6</sup> The results indicate that inside the sol–gel glass the liquids ( $\text{CS}_2$ , nitrobenzene,  $\text{CH}_3\text{CN}$ ,  $\text{CH}_3\text{I}$  etc) exhibits a major bulklike component whereas the liquid molecules attached to the silica surface of the glass display a component that is nearly 4 times slower.<sup>5</sup>

In bulk water, the major component ( $\sim 65\%$ ) of solvation dynamics is  $<0.1$  ps with a minor (35%) component of about 1 ps.<sup>9</sup> However, water molecules confined in many organized and constrained media exhibit a component that is slower by 2–3 orders of magnitude.<sup>10–16</sup> Bright and co-workers studied the solvation dynamics of water around a protein labeled with acrylodan in a sol–gel glass and reported a nanosecond component of solvation dynamics that is much slower than that in bulk water.<sup>11</sup> We studied solvation dynamics in a sol–gel matrix using coumarin 480 (C480, Scheme 1) as a fluorescence probe.<sup>12</sup> The emission maximum of C480 shifts from 407 nm in cyclohexane to 490 nm in water.<sup>17</sup> In a TEOS sol–gel matrix, the emission maximum of C480 is at 480 nm.<sup>12</sup> This indicates

## SCHEME 1: Structure of Coumarin 480 (C480)



that the microenvironment inside the sol–gel matrix is highly polar and protic. The solvation dynamics of C480 in the sol–gel matrix is described by two components of 120 ps (85%) and 800 ps (15%) and a total dynamic Stokes shift of 400  $\text{cm}^{-1}$ .<sup>12</sup> Baumann et al.<sup>13</sup> studied the solvation dynamics of ethanol using Nile blue and coumarin 153 (C153) as probes in sol–gel matrixes of different pore sizes. They found that for Nile blue<sup>13a</sup> the average solvation time of ethanol increases from 18.6 ps in 75-Å pores to 39 ps in 50-Å pores whereas for C153<sup>13b</sup> the average solvation time increases from 28.6 ps in 50-Å pores to 36.9 ps in 25-Å pores.

Most recently, we reported on the solvation dynamics in an ormosil using C480 as a probe. For this purpose, we used a sol–gel matrix doped with dimyristoyl-phosphatidylcholine (DMPC).<sup>14</sup> It is observed that the solvation dynamics in a DMPC-doped sol–gel matrix is very different from that in a DMPC lipid vesicle<sup>15</sup> in water or that in a sol–gel matrix.<sup>12</sup> For DMPC-doped sol–gel glass, the solvation dynamics displays two components of 90 ps (80%) and 2150 ps (20%) with a dynamic Stokes shift of 450  $\text{cm}^{-1}$ . The time constants of the solvation dynamics of C480 in a DMPC-entrapped sol–gel matrix ( $\langle\tau_s\rangle = 500$  ps) is about 14 times faster than that in a DMPC liposome in bulk water.<sup>15</sup>

Ferrer et al. recently studied the polarity and microviscosity of a cetyltrimethylammonium bromide (CTAB)-doped sol–gel matrix using phase fluorimetry and C153 as a probe.<sup>3b</sup> In this work, we report on the solvation dynamics in a sol–gel matrix doped with CTAB using C480 as a fluorescence probe.

## 2. Experimental Section

C480 (Exciton, laser grade), tetraethyl orthosilicate (TEOS) (Fluka, Purum grade), CTAB (Aldrich), and ethanol (Changshu Yangyuan Chemical, China) were used as received. The ormosil was prepared by mixing a solution of 1 mL of TEOS, 0.3 mL of doubly distilled deionized water, 0.7 mL of a solution of

\* Corresponding author. E-mail: pckb@mahendra.iacs.res.in. Fax: (91)-33-2473-2805.

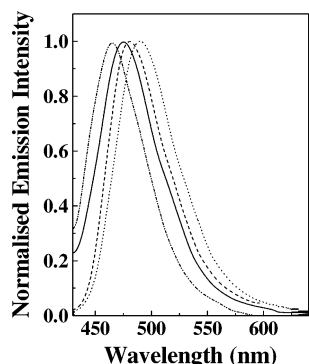


**Figure 1.** Steady-state emission spectra of C480 ( $\lambda_{\text{ex}} = 405$  nm) in (i) the CTAB-doped sol-gel matrix (— · —), (ii) CTAB micelles (—), (iii) the TEOS-derived sol-gel matrix (— —), and (iv) water (···).

C480 in ethanol, and 207 mg of CTAB. The total volume of the solution was 2 mL. The polymerization was carried out at room temperature in a quartz tube covered with aluminum foil. After gelation occurred, the aluminum foil was perforated to allow for the slow evaporation of solvents until dried ormosil was formed. The fluorescence experiments were done with a substantially aged semitransparent sol-gel composite after 30 days.

The steady-state absorption and emission spectra were recorded in a Shimadzu UV-2401 spectrophotometer and a Perkin-Elmer 44B spectrofluorimeter, respectively.

For lifetime measurements, the samples were excited at 405 nm using a picosecond diode laser (IBH Nanoled-07) of pulse width  $\sim 70$  ps at a repetition rate of 800 kHz. The fluorescence was dispersed using a monochromator (Applied Photophysics,  $f = 3.4$ ). To get time-resolved emission spectra, 10 decays were recorded at an interval of 10–15 nm using a 5-nm slit width. The exciting laser beam (at 405 nm) scattered by the sol-gel sample was blocked using a Melles Griot filter. The fluorescence decays were collected at a magic angle polarization using an analyzer and a Hamamatsu MCP photomultiplier (2809U). The time-correlated single-photon counting (TCSPC) setup consists of an Ortec 935 QUAD CFD and a Tennelec TC 863 TAC. The data are collected with a PCA3 card (Oxford) as a multichannel analyzer. The typical fwhm of the system response is about 100 ps. The fluorescence decays were deconvoluted using global lifetime analysis software (Photon Technology International) in which both the lifetimes and amplitudes of the individual decays were allowed to vary freely. To record the long-lifetime components ( $\sim 5$  ns), we recorded fluorescence decays up to 48 ns (full scale).

To study fluorescence anisotropy decay, the analyzer was rotated at regular intervals to get perpendicular ( $I_{\perp}$ ) and parallel ( $I_{\parallel}$ ) components ( $\lambda_{\text{em}} = 450$  nm). Then the anisotropy function,  $r(t)$  was calculated using the equation

$$r(t) = \frac{I_{\parallel}(t) - GI_{\perp}(t)}{I_{\parallel}(t) + 2GI_{\perp}(t)} \quad (1)$$

The  $G$  value of the setup was determined using a probe whose rotational relaxation is very fast (e.g., Nile red in methanol), and the  $G$  value was found to be 1.

### 3. Results

**3.1. Steady-State Emission Spectrum of C480 in a CTAB-Doped Sol-Gel Matrix.** Figure 1 shows the emission spectrum of C480 in a sol-gel matrix doped with CTAB. It is readily seen that the emission maximum of C480 in this medium is at

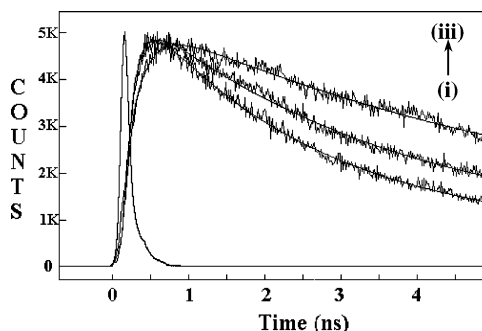


**Figure 2.** Fluorescence decays of C480 in the CTAB-doped sol-gel matrix at (i) 435 nm, (ii) 455 nm, and (iii) 530 nm.

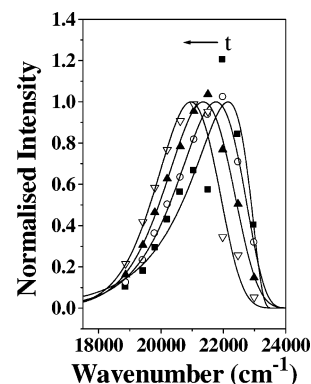


**Figure 3.** Time-resolved emission spectra of C480 in the CTAB-doped sol-gel matrix at 0 ps (■), 500 ps (○), 5000 ps (▲), and 20 000 ps (▽).

465 nm (Figure 1). For a comparison of the emission spectra of C480 in water, CTAB micelles and the TEOS sol-gel matrix are also shown in the same Figure. It may be recalled that the emission maximum of C480 is at 480 nm in a sol-gel matrix<sup>12</sup> and at 475 nm in a CTAB micelle.<sup>16</sup> It is evident that there is a marked blue shift in the emission maximum of C480 in a CTAB-doped sol-gel matrix compared to that in a sol-gel matrix and in CTAB micelles. This indicates that the micro-environment inside the CTAB-doped sol-gel matrix is less polar than that in the sol-gel matrix and CTAB micelles. The position of the emission maximum (465 nm) of C480 indicates that the polarity of the CTAB-doped sol-gel matrix is intermediate between that of ethanol (emission maximum at 473 nm) and that of acetonitrile (450 nm).<sup>17</sup>

**3.2. Time-Resolved Studies: Solvation Dynamics.** In a CTAB-doped sol-gel matrix, C480 exhibits wavelength-dependent emission decays with growth at the red end and decay at the blue end. This is typical of a probe displaying solvation dynamics. Figure 2 displays the initial part of the fluorescence decays at 3 (out of 10) wavelengths. In this case, at the blue end (435 nm) the decay is fit to a biexponential with two components of 1.98 ns (78%) and 4.33 ns (22%) (Figure 2). However, at the red end (e.g., at 530 nm), C480 in the CTAB-doped sol-gel matrix exhibits a distinct rise of 250 ps followed by a decay component of 5.4 ns (Figure 2). Following Fleming and Maroncelli,<sup>18</sup> the time-resolved emission spectra (TRES) were constructed using the parameters of best fit to the fluorescence decays and the steady-state emission spectrum. The TRES show a time-dependent Stokes shift (Figure 3). The solvation dynamics is described by the decay of the solvent correlation function  $C(t)$ , defined as

$$C(t) = \frac{\nu(t) - \nu(\infty)}{\nu(0) - \nu(\infty)} \quad (2)$$

**TABLE 1: Decay Parameters of  $C(t)$  of C480 in Different Systems**

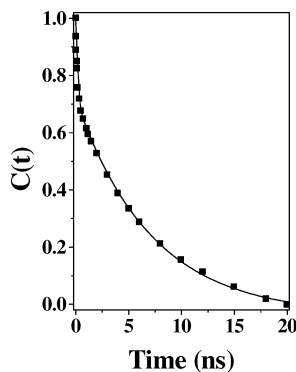
system	$\Delta\nu^a$ (cm <sup>-1</sup> )	$a_1$	$\tau_1^b$ (ps)	$a_2$	$\tau_2^b$ (ps)	$\langle\tau_s\rangle^{b,c}$ (ps)
CTAB doped sol–gel matrix	1200	0.25	120	0.75	7200	5430
CTAB micelle <sup>d</sup>	490	0.40	285	0.60	600	475
TEOS derived sol–gel matrix <sup>e</sup>	400	0.85	120	0.15	800	220

<sup>a</sup>  $\pm 100$  cm<sup>-1</sup>. <sup>b</sup>  $\pm 10\%$ . <sup>c</sup>  $\langle\tau_s\rangle = a_1\tau_1 + a_2\tau_2$ . <sup>d</sup> Reference 16. <sup>e</sup> Reference 12.

**TABLE 2: Parameters of the Anisotropic Decay of C480 (at 450 nm) in a CTAB-Doped Sol–Gel Matrix**

system	$r_0$	$r_\infty$	$a_{\text{fast}}^a$	$\tau_{\text{fast}}^a$ (ps)	$a_{\text{slow}}^a$	$\tau_{\text{slow}}^a$ (ps)	$\langle\tau_s\rangle^{a,b}$ (ps)
CTAB doped sol–gel matrix	0.24	0.12	0.75	90	0.25	600	220

<sup>a</sup>  $\pm 5\%$ . <sup>b</sup>  $\langle\tau_s\rangle = a_{\text{fast}}\tau_{\text{fast}} + a_{\text{slow}}\tau_{\text{slow}}$ .

**Figure 4.** Decay of response function,  $C(t)$ , of C480 in the CTAB-doped sol–gel matrix. The points denote the actual values of  $C(t)$ , and the solid line denotes the best fit to a biexponential decay.

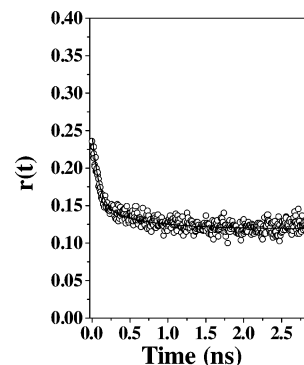
where  $\nu(0)$ ,  $\nu(t)$ , and  $\nu(\infty)$  are the peak frequencies at times 0,  $t$ , and  $\infty$ , respectively. The decay of  $C(t)$  is shown in Figure 4, and the decay parameters are summarized in Table 1. The decay of  $C(t)$  for C480 in the CTAB-doped sol–gel matrix is found to be biexponential with one component of 120 ps (25%) and another of 7200 ps (75%), with an average solvation time of  $\langle\tau_s\rangle = 5430$  ps (Table 1). The total Stokes shift is observed to be  $1200 \pm 100$  cm<sup>-1</sup>. The decay parameters of  $C(t)$  for C480 in the sol–gel matrix<sup>12</sup> and in CTAB micelles<sup>16</sup> are also listed in Table 1. It is readily seen that the solvation dynamics in the CTAB-doped sol–gel matrix is much slower compared to that in the sol–gel matrix (major component 120 ps)<sup>12</sup> and in CTAB micelles in bulk water ( $\langle\tau_s\rangle = 475$  ps).<sup>16</sup>

The dynamic Stokes shift of C480 observed in the case of the sol–gel matrix<sup>12</sup> (400 cm<sup>-1</sup>) or CTAB micelles<sup>16</sup> (490 cm<sup>-1</sup>) is much smaller than that obtained in the present case. This shows that a greater amount of the solvation dynamics of C480 is captured in the case of the CTAB-doped sol–gel matrix in our setup with a time resolution 100 ps.

**3.3. Fluorescence Anisotropy Decay.** The fluorescence anisotropy decay of C480 in the CTAB-doped sol–gel matrix exhibits a residual anisotropy of 0.12. The anisotropy decay is fit to a hindered rotor as

$$r(t) - r(\infty) = \{r(0) - r(\infty)\} \left[ a_{\text{fast}} \exp\left(-\frac{t}{\tau_{\text{fast}}}\right) + a_{\text{slow}} \exp\left(-\frac{t}{\tau_{\text{slow}}}\right) \right] \quad (3)$$

The time constants for the decay of  $r(t)$  are found to be 90 ps (75%) and 600 ps (25%) (Table 2). Figure 5 shows the fluorescence anisotropy decay of C480 in the CTAB-doped sol–gel matrix. The high residual anisotropy value (0.12) indicates that the rotation of the C480 probe is constrained inside the

**Figure 5.** Raw data along with the fitted curve describing the fluorescence anisotropy decay of C480 in the CTAB-doped sol–gel matrix.

CTAB-doped sol–gel glass. It may be recalled that Ferrer et al. also reported a high residual anisotropy ( $>0.2$ ) in a CTAB-doped sol–gel glass. For a DMPC-doped sol–gel glass, we earlier detected a residual anisotropy of 0.08.<sup>14</sup>

The fluorescence anisotropy decays in a micelle in aqueous solutions are usually analyzed in terms of the “wobbling-in-cone” model.<sup>19</sup> According to this model, the decay of fluorescence anisotropy is a product of three independent motions: (i) wobbling of the probe,  $r_w(t)$ , with a time constant  $\tau_R$ , (ii) translation of the probe along the surface of the micelle,  $r_t(t)$ , with a time constant  $\tau_D$ , and (iii) overall rotation of the micelle,  $r_M(t)$ , with a time constant  $\tau_M$ .<sup>19</sup>

$$r(t) - r(\infty) = r_w(t) r_t(t) r_M(t) \quad (4)$$

By comparing eqs 3 and 4, one immediately obtains

$$\frac{1}{\tau_{\text{fast}}} = \frac{1}{\tau_R} + \frac{1}{\tau_D} + \frac{1}{\tau_M} \quad (5)$$

$$\frac{1}{\tau_{\text{slow}}} = \frac{1}{\tau_D} + \frac{1}{\tau_M} \quad (6)$$

When the probe is attached to a spherical particle,  $\tau_M$  is given by<sup>19</sup>

$$\tau_M = \frac{4\pi\eta r_h^3}{3kT} \quad (7)$$

where  $\eta$  is the viscosity of water and  $r_h$  is the hydrodynamic radius of the spherical micelle. According to SANS studies, for CTAB micelles  $r_h \approx 40$  Å.<sup>20</sup> Thus, at 20 °C the time constant of overall rotation of the micelle is  $\tau_M \approx 65\,000$  ps (65 ns). Evidently, the contribution of the overall rotation of CTAB micelles is negligible in the observed decay components of 90 and 600 ps. We calculated that the time constant of wobbling is  $\tau_R \approx 100$  ps and the time constant of translation is  $\tau_D \approx 600$



ps. The high residual anisotropy may originate from hindered rotation of the C480 probe molecule at the silica-CTAB interface and the very long overall rotational time of CTAB micelles (65 ns).

#### 4. Discussion

The most interesting finding of the present work is the dramatic retardation of solvation dynamics in a CTAB-doped sol-gel composite compared to that in an ordinary CTAB micelle<sup>16</sup> or a sol-gel glass alone.<sup>12</sup> It is evident that the C480 probe experiences a very different microenvironment inside the CTAB-doped sol-gel matrix, which resembles neither the sol-gel matrix<sup>12</sup> nor the CTAB micelle in bulk water.<sup>16</sup> From the position of the emission maximum of C480, the polarity of the CTAB-doped sol-gel glass is estimated to be intermediate between that of acetonitrile and ethanol.

The average solvation time of C480 in the CTAB-doped sol-gel matrix ( $\langle\tau_s\rangle = 5430$  ps) is about 12 times slower than that in CTAB micelles in bulk water.<sup>16</sup> This demonstrates that the water molecules in the ormosil are much slower than those in a CTAB micelle.<sup>16</sup> The solvation dynamics of C480 in CTAB-doped ormosil is very different from that in the sol-gel matrix. The fast component (120 ps) of the solvation dynamics of C480 in a CTAB-doped sol-gel matrix is identical to the major component of solvation dynamics (120 ps) of C480 in a sol-gel matrix.<sup>12</sup> However, the ultraslow component (7200 ps) detected in the case of the CTAB-doped sol-gel glass is absent in a sol-gel matrix.<sup>12</sup>

The anisotropy decay and the high residual anisotropy (0.12) indicate that the microenvironment of the fluorescence probe (C480) is markedly hindered inside the CTAB-doped sol-gel composite. Ferrer et al. attributed the high value of residual anisotropy and the long rotational relaxation time of C153 in a CTAB-doped sol-gel matrix to the strong binding of CTAB micelles to the silica surface and to the restricted motion of the probe (C153) at the silica-CTAB interface.<sup>3b</sup>

The anisotropy decay of C480 in the CTAB-doped sol-gel matrix displays similar high residual anisotropy that may arise from the very slow overall rotation of CTAB micelles ( $\tau_M \approx 65\,000$  ps). We have analyzed the anisotropy decay using the "wobbling-in-cone" model and have calculated the time constants for wobbling and translation of the fluorescence probe (C480). According to our analysis, at the silica-CTAB interface the C480 probe exhibits fast wobbling motion ( $\tau_R \approx 100$  ps) and translational diffusion with a time constant of 600 ps.

It is obvious that the time constant of overall rotation of CTAB micelles is far too long to explain the long component of the solvation dynamics (7200 ps) of the CTAB-doped sol-gel matrix. It should also be noted that the solvation dynamics of C480 in CTAB micelles in bulk water exhibits two components of 285 ps (40%) and 600 ps (60%).<sup>16</sup> These components are much faster than the time constant of overall rotation of the micelles. Thus, it is evident that the overall rotation of CTAB micelles inside the sol-gel matrix is not responsible for the very slow component of solvation dynamics of CTAB micelles either in bulk water or in the sol-gel matrix.

The cationic CTAB micelle is expected to bind strongly to the silica surface for the following reason. At low pH, the silica surface consists of Si-OH groups, but at high pH, they are converted to Si-O<sup>-</sup>. Eisenthal and co-workers studied the variation in charge of the silica surface using surface second-harmonic generation.<sup>21</sup> They suggested that there exist two types of Si-OH moieties. One of them is converted to Si-O<sup>-</sup> at pH 4.5, and both are converted to Si-O<sup>-</sup> at pH > 12. In our case,

the hydrolysis is carried out at neutral pH (7). At this pH, the surface consists of both Si-OH and Si-O<sup>-</sup> moieties, and the cationic surfactant CTAB binds strongly to both Si-O<sup>-</sup> and Si-OH.

In summary, we ascribe the ultraslow component of solvation (7200 ps) to the adsorption of CTAB micellar aggregates on the silica surface. The movement of the water molecules is highly restricted at the silica-CTAB interface because of the formation of hydrogen bonds with the silica surface as well as the polar headgroups of CTAB. It seems that the majority (75%) of the probe molecules (C480) resides at the silica-CTAB interface and hence exhibits a very long component of 7200 ps. A minor fraction (25%) of the probe molecules seem to be located at a distance from CTAB inside the sol-gel matrix that has a relatively fast component of 120 ps, which is identical to the major (85%) component of solvation dynamics of C480 in a TEOS sol-gel matrix.<sup>12</sup>

#### 5. Conclusions

This work demonstrates that the presence of CTAB in the sol-gel matrix affects the dynamics of water molecules inside it. The solvation dynamics of C480 in the CTAB-doped sol-gel matrix is about 12 times slower than that in CTAB micelles in bulk water. The ultraslow solvation dynamics may be ascribed to the restriction imposed on the motion of the water molecules entrapped between the polar headgroups of the CTAB molecules and the silica surface. The large residual anisotropy (0.12) in the CTAB-doped sol-gel matrix may be due to hindered rotation of the C480 probe molecule at the silica-CTAB interface and very slow overall rotation of CTAB micelles.

**Acknowledgment.** Thanks are due to the Department of Science and Technology of India, the Femtosecond Laser Facility, and the Council of Scientific and Industrial Research (CSIR) for generous research grants. K.S., D.R., S.K.M., and A.H. thank the CSIR for awarding fellowships.

#### References and Notes

- (1) (a) Gill, I. *Chem. Mater.* **2001**, *13*, 3404. (b) Brinker, C. J.; Scherer, G. W. *Sol-Gel Science*; Academic Press: New York, 1990.
- (2) (a) Brennan, J. D.; Benjamin, D.; DiBattista, E.; Gulcev, M. D. *Chem. Mater.* **2003**, *15*, 737. (b) Besanger, T. R.; Chen, Y.; Deisingh, A. K.; Hodgson, R.; Jin, W.; Mayer, S.; Brook, M. A.; Brennan, J. D. *Anal. Chem.* **2003**, *75*, 2382. (c) Brook, M. A.; Chen, Y.; Guo, K.; Zhang, Z.; Brennan, J. D. *J. Mater. Chem.* **2004**, *14*, 1469. (d) Goring, G.; Brennan, J. D. *J. Mater. Chem.* **2002**, *12*, 3400. (e) Besanger, T.; Zhang, Y.; Brennan, J. D. *J. Phys. Chem. B* **2002**, *106*, 10535.
- (3) (a) Ferrer, M. L.; del Monte, F.; Levy, D. *Chem. Mater.* **2002**, *14*, 3619. (b) Ferrer, M. L.; del Monte, F.; Levy, D. *J. Phys. Chem. B* **2001**, *105*, 11076. (c) del Monte, F.; Ferrer, M. L.; Levy, D. *J. Mater. Chem.* **2001**, *11*, 1745. (d) Levy, D.; Avnir, D. *J. Phys. Chem.* **1988**, *92*, 4734.
- (4) (a) Narang, U.; Prasad, P. N.; Bright, F. V.; Kumar, A.; Kumar, N. D.; Malhotra, B. D.; Kamalasanan, M. N.; Chandra, S. *Anal. Chem.* **1994**, *66*, 3139. (b) Narang, U.; Prasad, P. N.; Bright, F. V.; Kumar, A.; Kumar, N. D.; Malhotra, B. D.; Kamalasanan, M. N.; Chandra, S. *Chem. Mater.* **1994**, *6*, 1596. (c) Narang, U.; Jordan, J. O.; Bright, F. V.; Prasad, P. N. *J. Phys. Chem.* **1994**, *98*, 8101.
- (5) (a) Farrer, R. A.; Fourkas, J. T. *Acc. Chem. Res.* **2003**, *36*, 605. (b) Loughnane, B. J.; Farrer, R. A.; Scodinu, A.; Reilly, T.; Fourkas, J. T. *J. Phys. Chem. B* **2000**, *104*, 5421.
- (6) (a) Warnock, J.; Awschalom, D. D.; Shafer, M. W. *Phys. Rev. Lett.* **1986**, *57*, 1753. (b) Warnock, J.; Awschalom, D. D.; Shafer, M. W. *Phys. Rev. B* **1986**, *34*, 475. (c) Warnock, J.; Awschalom, D. D.; Shafer, M. W. *Phys. Rev. B* **1987**, *35*, 1962.
- (7) (a) Korb, J.-P.; Xu, S.; Cros, F.; Malier, L.; Jonas, J. J. *Chem. Phys.* **1997**, *107*, 4044. (b) Xu, S.; Jonas, J. J. *J. Phys. Chem.* **1996**, *100*, 16242.
- (8) Yang, M.; Richert, R. *J. Phys. Chem. B* **2003**, *107*, 895.
- (9) (a) Jarzeba, W.; Walker, G. C.; Johnson, A. E.; Kahlow, M. A.; Barbara, P. F. *J. Phys. Chem.* **1988**, *92*, 7039. (b) Jimenez, R.; Fleming, G.

R.; Kumar, P. V.; Maroncelli, M. *Nature* **1994**, 369, 471. (c) Nandi, N.; Roy, S.; Bagchi, B. *J. Chem. Phys.* **1995**, 102, 1390.

(10) (a) Bhattacharyya, K. *Acc. Chem. Res.* **2003**, 36, 95. (b) Nandi, N.; Bhattacharyya, K.; Bagchi, B. *Chem. Rev.* **2000**, 100, 2013. (c) Bhattacharyya, K.; Bagchi, B. *J. Phys. Chem. A* **2000**, 104, 10603. (d) Pal, S. K.; Peon, J.; Bagchi, B.; Zewail, A. H. *J. Phys. Chem. B* **2002**, 106, 12376.

(11) Jordan, J. D.; Dunbar, R. A.; Bright, F. V. *Anal. Chem.* **1995**, 67, 2436.

(12) Pal, S. K.; Sukul, D.; Mandal, D.; Sen, S.; Bhattacharyya, K. *J. Phys. Chem. B* **2000**, 104, 2613.

(13) (a) Baumann, R.; Ferrante, C.; Deeg, F.-W.; Brauchle, C. *J. Chem. Phys.* **2001**, 114, 5781. (b) Baumann, R.; Ferrante, C.; Kneuper, E.; Deeg, F.-W.; Brauchle, C. *J. Phys. Chem. A* **2003**, 107, 2422.

(14) Halder, A.; Sen, S.; Das Burman, A.; Patra, A.; Bhattacharyya, K. *J. Phys. Chem. B* **2004**, 108, 2309.

(15) Datta, A.; Pal, S. K.; Mandal, D.; Bhattacharyya, K. *J. Phys. Chem. B* **1998**, 102, 6114.

(16) Sarkar, N.; Datta, A.; Das, S.; Bhattacharyya, K. *J. Phys. Chem.* **1996**, 100, 15483.

(17) Jones, G., II; Jackson, W. R.; Choi, C. Y.; Bergmark, W. R. *J. Phys. Chem.* **1985**, 89, 294.

(18) Maroncelli, M.; Fleming, G. R. *J. Chem. Phys.* **1987**, 86, 6221.

(19) (a) Wittouck, N. W.; Negri, R. M.; De Schryver, F. C. *J. Am. Chem. Soc.* **1994**, 116, 10601. (b) Quitevis, E. L.; Marcus, A. H.; Fayer, M. D. *J. Phys. Chem.* **1993**, 97, 5762. (c) Sen, S.; Sukul, D.; Dutta, P.; Bhattacharyya, K. *J. Phys. Chem. B* **2001**, 105, 7495. (d) Krishna, M. G. M.; Das, R.; Periasamy, N.; Nityananda, R. *J. Chem. Phys.* **2000**, 112, 8502.

(20) Berr, S. S. *J. Phys. Chem.* **1987**, 91, 4760.

(21) Ong, S.; Zhao, X.; Eisinger, K. B. *Chem. Phys. Lett.* **1992**, 191, 327.